

High-gradient acceleration of electron beam by superradiative microwave pulse

K.A. Sharypov^{1,}, N.S. Ginzburg², V.G. Shpak¹, S.A. Shunailov¹, M.I. Yalandin¹, I.V. Zotova²*

¹*Institute of Electrophysics UB RAS, Yekaterinburg, Russia*

²*Institute of Applied Physics RAS, Nizhny Novgorod, Russia*

**const@iep.uran.ru*

Abstract. For high-gradient acceleration of electron bunches by microwave superradiance pulses, a scheme is considered in which devices for the radiation generation and particle acceleration are combined. Two electron beams from coaxial cathodes powered by a single voltage pulse (-300 kV; 1.5 ns) are used. Outer tubular beam excites a relativistic superradiant Ka-band backward-wave oscillator (BWO), and paraxial beam is accelerated in a “pill-box” cavity positioned at the input of the BWO slow-wave structure. Formation of such beams is studied with the use a model cathode system. In calculations by particles-in-cells method, the rate of electron acceleration of up to 400 MeV/m was obtained and the role of nonsynchronous microwaves-to-bunches interaction was shown.

Keywords: superradiance, coaxial beams, acceleration.

1. Introduction

Interest in high-gradient electron acceleration by subgigawatt Ka-band superradiance (SR) pulses is because such pulses are shorter than 300 ps. With such small exposure of strong microwave fields, breakdown of electrodynamic structures can be delayed even in a technical vacuum. For example, in relativistic Ka-band backward wave oscillators (BWO), it is possible to obtain SR pulses with a power of $1-3$ GW [1–3], although the microwave electric field strength on the wall of a slow-wave structure (SWS) exceeds 2 MV/cm. Below, in the development of the method [4], we consider acceleration of a paraxial electron beam in a low-Q “pill-box” cavity. In calculations by particles-in-cells method within the KARAT code [5], the energy characteristics of accelerated bunches are analyzed using phase portraits of electron beam.

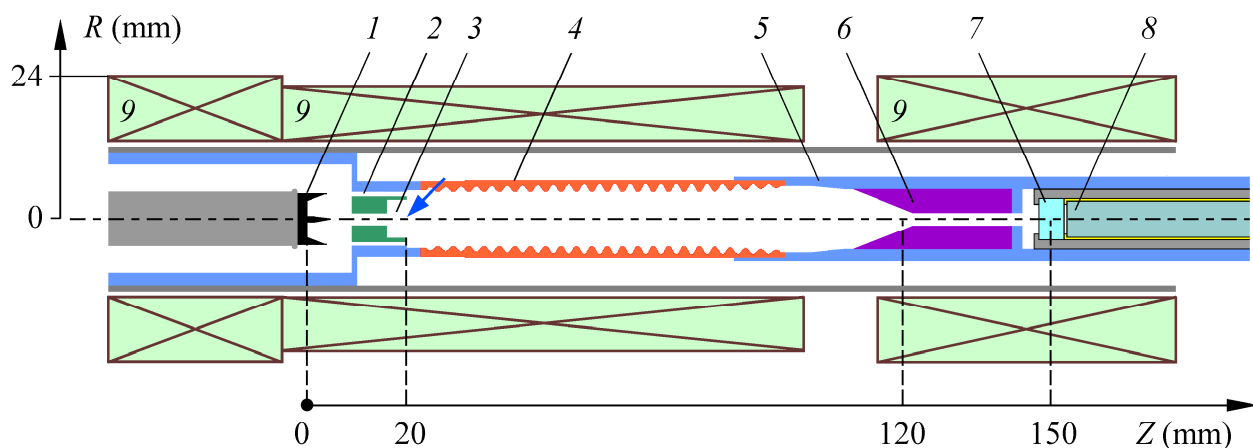


Fig.1. Design of united block proposed for SR pulse generation and high-gradient acceleration of a paraxial beam: 1 – coaxial graphite cathodes; 2 – round radial slot; 3 – pill-box cavity; 4 – SWS of SR BWO; 5 – collector of external beam; 6 – microwave absorber; 7 – Al-filter; 8 – collector of a fast-response beam probe; 9 – solenoid coils.

2. Experimental scheme and formation of coaxial beams

In contrast to [4], we consider a scheme where devices for SR generation and particle acceleration are combined in one block (Fig.1). This is possible if coaxial cathodes [6, 7] are used, which operate in the mode of explosive electron emission in a strong longitudinal magnetic field. To power the cathodes, one accelerating pulse is needed and, therefore, there is no problem of synchronization of the generator and accelerator sections of the installation. An external

(generating) tubular beam feeds SR BWO in which a resonant reflector at the SWS input is replaced by a low-Q “pill-box” cavity. By analogy with [8, 9], a narrow (0.5 mm) annular slot between the cavity and the wall of the anode constriction in front of SWS is used to transfer the beam into SWS. The central beam from a needle cathode passes through a paraxial hole of the cavity and is accelerated in a strong, longitudinal high-frequency field (TM₀₁ mode) that occurs when the cavity is pumped for a few microwave periods.

Paraxial beam current must be significantly less than external beam current in order to prevent reduction of the SR BWO generation power. This issue and possibility of adjusting the beam currents ratio were analyzed in the experiment with a prototype cathode system (Fig.2a). The currents of coaxial beams were registered by collector probe separately (in turn). In the case of the gap between the cathode and the anode constriction $D = 10$ mm, for a 1-ns accelerating pulse amplitude of -220 kV and an external tubular beam current of about 1 kA (Fig.2b), the change in protrusion of central needle cathode (δ) led to the paraxial beam current variations within 15–150 A (Fig.2c). When a needle cathode is deepened, electric field at its tip decreases, and together with the current drop at $\delta < 0$, a delay in the emission of paraxial beam of ~ 100 ps and more extended front are observed. These effects do not preclude the use of the paraxial beam for acceleration since SR pulse pumps the cavity approximately 1 ns after the start of the generating beam emission. Therefore, accelerating pulse and beam currents should be approximately twice as long as in Fig.2.

The second series of experiments with coaxial electron beams was performed using SR BWO operating in a 38 GHz band [10]. Gap D was reduced to 6 mm, and an external beam current increased to ≈ 2.2 kA. At the position of a needle cathode $\delta = 0$, a paraxial beam current was 60 A, and this increase is also associated with a decrease in the gap D . With a longitudinal magnetic field induction of ≈ 2 T, paraxial beam represented a jet with a diameter of about 0.5 mm at the SWS entrance (Fig.2d). The radial field of TM₀₁ wave decreases towards the axis, and therefore, despite the high SR power (at least 400 MW), the imprint of paraxial beam at the SWS output broadened to no more than 1 mm in diameter (Fig.2e). A probable reason for the broadening was specific configuration of magnetic field lines. This field falls towards collector of external beam, in front of which the beam imprint was recorded.

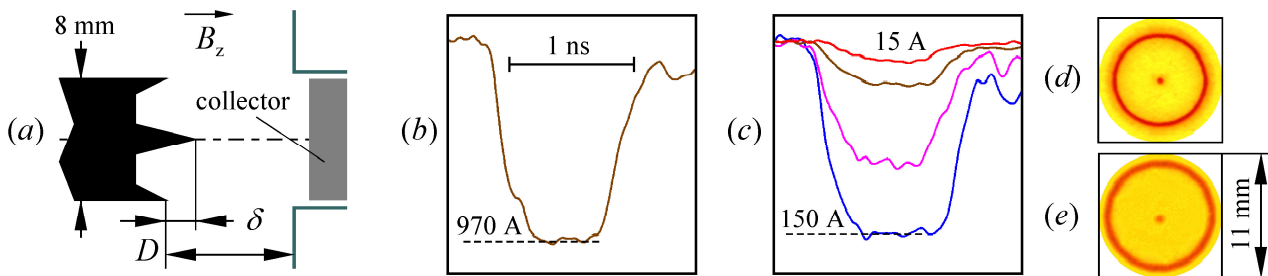


Fig.2. (a) Electron injector with coaxial cathodes. (b) Current pulse of an external tubular beam. (c) Currents of paraxial beam depending on protrusion δ : 150 A for $\delta = +2$ mm; 15 A for $\delta = -1.6$ mm. (d) and (e) Reprints of coaxial beams obtained for SR BWO before and after SWS, consequently.

3. Numerical experiment on high-gradient electron acceleration by SR pulse

Numerical model geometry [5] for calculating an axially symmetric problem for acceleration of paraxial beam by SR pulse corresponds to the construction shown in Fig.1. Computational grid along the R - Z coordinates had a discreteness of 0.1 mm. Fig.3a shows the shape of accelerating pulse at the cathode with an amplitude of $U \approx -300$ kV and a full width at half maximum (FWHM) of ≈ 1.5 ns. When the transit channel of external beam is closed, the only paraxial beam current is observed after the cavity (≈ 250 A in Fig.3b). The phase portrait of this beam is shown in Fig.3c as an ensemble of the particles colored in red. Normalized longitudinal momentum of electrons is

$P_z/mc \approx 1.1$, and this corresponds to the beam kinetic energy of ≈ 250 keV. Here m is the total electron mass; c is the speed of light. Some decrease in the energy compared to eU (e is the electron charge) is partly determined by the small beam diameter when the “potential sag” increases. An outer tubular beam with the current of ≈ 2.2 kA in a strong magnetic field $B_z \approx 7$ T (Fig.3d) passes near SWS wall, and its phase portrait at the SWS entrance (this is an ensemble of blue macroparticles in Fig.3c) corresponds to the energy of ≈ 275 keV. Note that the axial gap between solenoid windings (Fig.1) ensures the dip of magnetic field in the area of an external beam collector, i.e., ensures its drop onto the wall at $z \approx 110$ mm. Paraxial beam expands somewhat in this area, but then contracts again in a strong field (Fig.3d) and is delivered in this form to the collector of the current probe. In a real experiment, aluminum disk will be placed in front of collector. This is a filter that passes only a fraction of electrons with energy above a certain value.

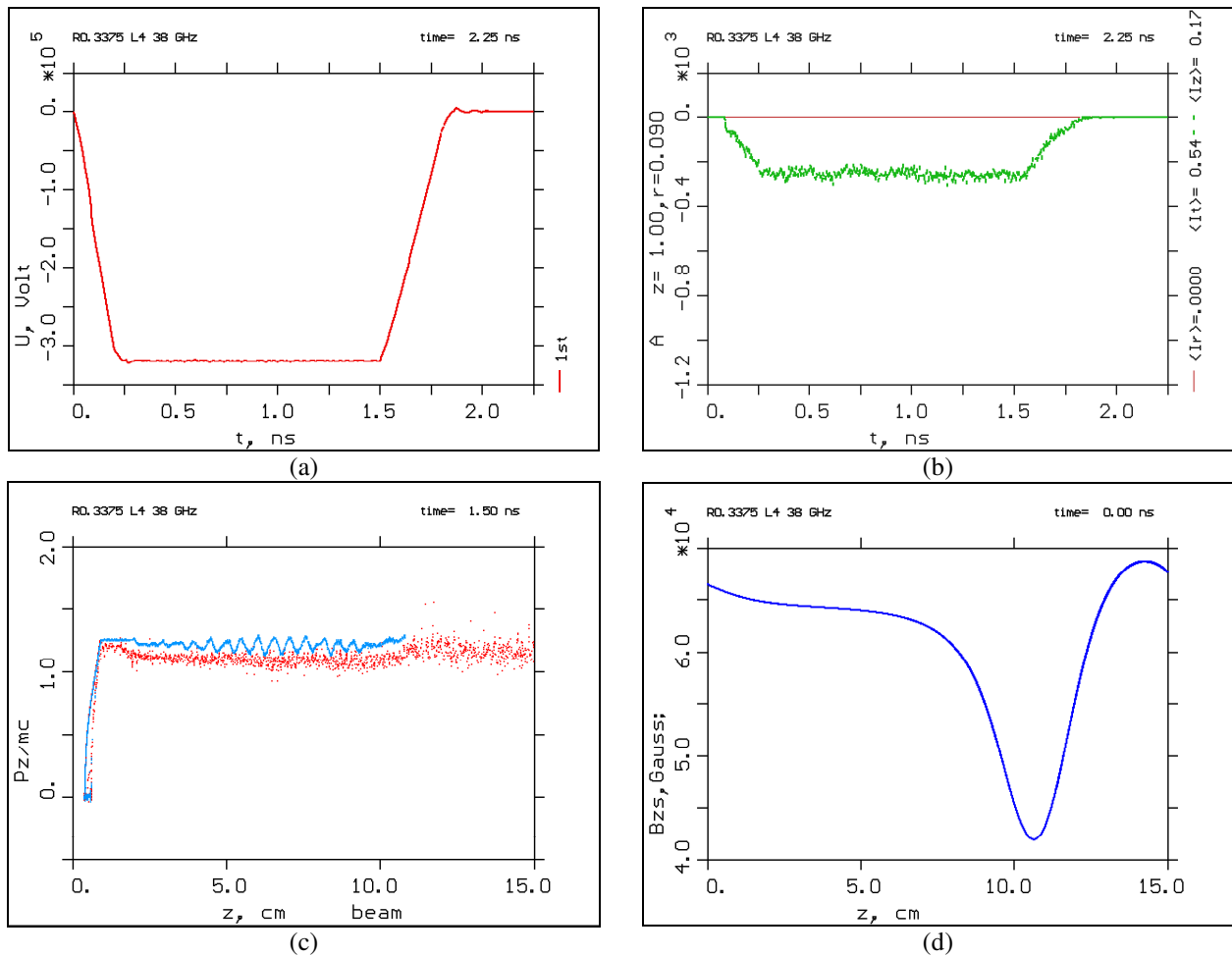


Fig.3. Numerical model. (a) Accelerating voltage. (b) Current of paraxial beam and. (c) Normalized momentum of coaxial beams. (d) Distribution of guiding magnetic field at the axis. Detailed comments are given in the text.

When the reflector representing conductive cylinder with a flat end is installed instead of the cavity [8, 9], SR BWO generates the radiation pulse with a peak power of ≈ 800 MW (Fig.4a). In the presence of the cavity, at its input at the point $z = 20$ mm (see arrow in Fig.1), non-averaged power of SR pulse looks as it is shown in Fig.4b. There is a radiation pulse incident from right to left (negative polarity) with a peak power of about 1 GW. This is followed by a positive (reflected) pulse of smaller amplitude, and it is somewhat elongated after pumping the cavity. Fig.4c shows radio pulse at the point near axis in the cross section of a cavity bottom ($z = 16.1$ mm; $r = 0.1$),

which is a time dependence of the strength of longitudinal electric field of TM_{01} wave. At the pump maximum, the strength reaches ≈ 5 MV/cm at the time of ≈ 1.2 ns. Near this maximum, the phase portrait (Fig.4d) shows the bunch of accelerated electrons leaving the cavity, for which $P_z/mc \approx 4.5$, i.e., their kinetic energy is 1.85 MeV. Taking into account that initial energy of the paraxial beam was ≈ 250 keV, the energy gain was 1.6 MeV, and this was provided by acceleration inside the cavity with a depth of 4 mm. Thus, according to the terminology accepted in accelerator technology, an acceleration gradient has reached 400 MV/m. Let us note that the field in the cavity periodically changes sign, and therefore, along with accelerated bunches moving in the “+z” direction, a flow of particles accelerated in the opposite direction appears. This can be seen in Fig.4d as a group of particles in the interval $z < 20$ mm with a negative value of P_z/mc . These electrons then return to the cathode.

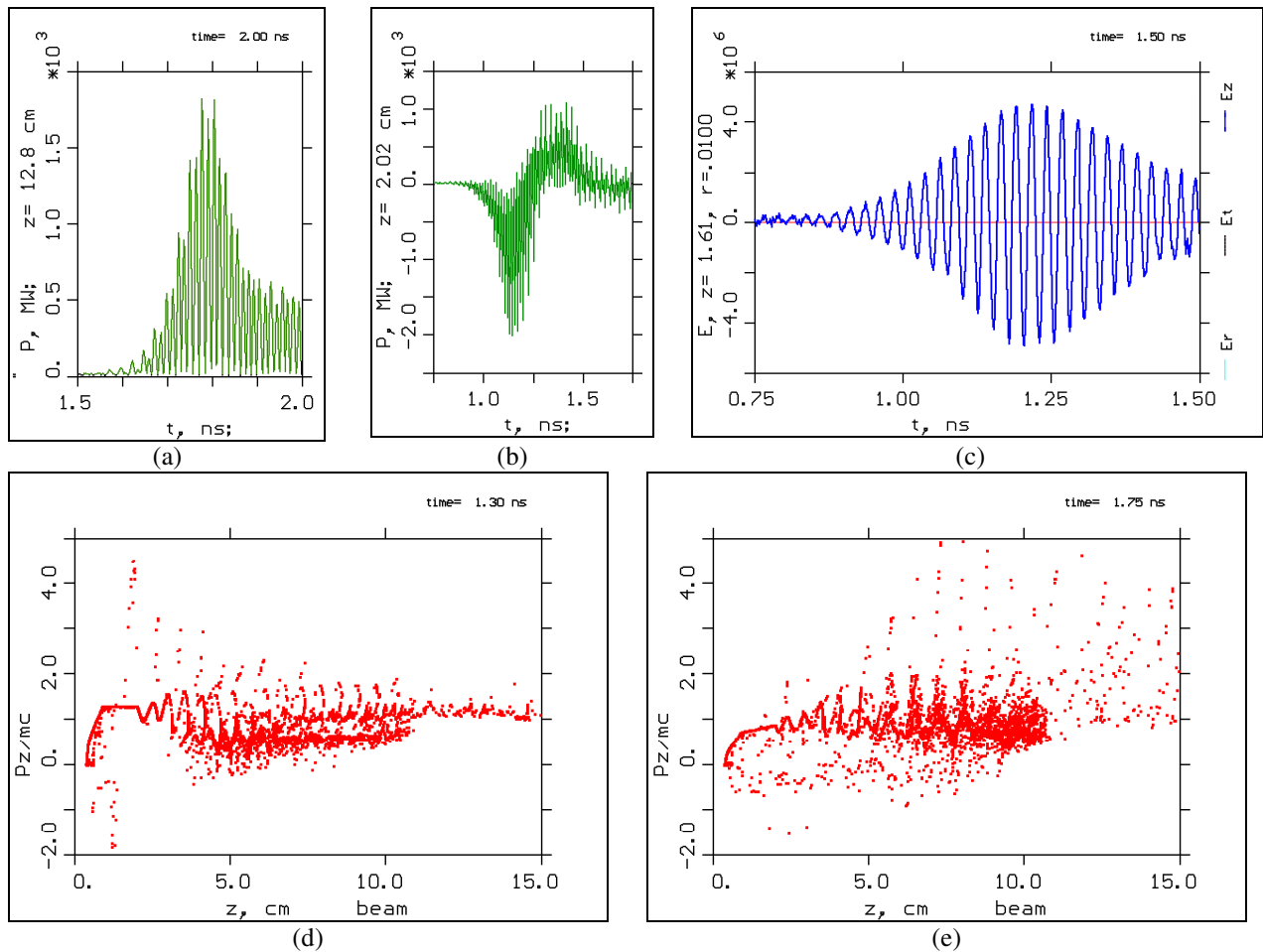


Fig.4. Numerical model. (a) Non-averaged power of SR pulse generated when a “pill-box” cavity was replaced with a flat reflector. (b) Non-averaged power of SR pulse at the “pill-box” entrance. (c) E_z -component of a pumping SR pulse (TM_{01}) in V/cm simulated for a paraxial point nearby the “pill-box” bottom. (d), (e) Phase portraits of accelerated bunches at the instants 1.3 and 1.75 ns. Detailed comments are given in the text.

In the region near maximum of the cavity pump field (Fig.4c), a sequence of bunches accelerated in “+z” direction is formed. Their further history is determined by the fact that this train is output along the SWS channel axis, and here the “used” SR pulse propagates along the way. Since the normalized velocity of accelerated electrons ($v/c \approx 0.98$) is much greater than the group velocity of SR wave packet (the latter is usually $< 0.5c$), fast electrons overtake the wave experiencing a periodic nonsynchronous action of sufficiently strong electric field of variable

direction. This takes place over entire region of the bunch motion up to the region of microwave absorption in the cross section $z = 120$ mm. As a result, at $z < 120$ mm, bunches periodically additionally gain and lose energy. Fig.4e shows that even very “late” paraxial beam electrons can be accelerated so that $P_z/mc \approx 5$, that is, their kinetic energy reaches 2.1 MeV. According to calculations, longitudinal electric field of SR pulse responsible for effect of nonsynchronous acceleration/deceleration has the maximum (amplitude) strength of $\approx \pm 1$ MV/cm at the axis in front of the microwave absorber. Since this value is much smaller than the field in the cavity, there is no flux of paraxial beam particles moving in “ $-z$ ” direction, and a periodical decrease in the bunch energy is relatively small. As a result, in the region $z > 120$ mm, where there is no SR pulse, the final bunch structure with a maximum energy of ≈ 1.6 MeV is observed (Fig.4e).

4. Conclusion

In conclusion, we note the features of a promising experimental implementation of the described scheme for high-gradient electron acceleration. First, according to calculations, the structure of paraxial beam after collector of an external beam ($z > 110$ mm, Fig.1) represents a fairly regular bunch sequence with a period of ≈ 26 ps corresponding to Ka-band SR pulse. It is supposed to register these particles in a real time using collector probe similar to that described in [11]. It was shown here that, using an oscilloscope with a proper registration bandwidth, one can register a single electron bunch with duration of ≈ 10 ps (FWHM). Problem of registering a sequence of such bunches when low-energy particles are cut off by a filter is of special interest. The second problem is the probability of breakdown development at the “singularity” points of electrodynamic system. First of all, these are 90-degree edges of the cavity. When pumping with a subgigawatt Ka-band SR pulse (Fig.4b), the field strengths of ≈ 5 MV/cm can be achieved near the cavity critical points. However, these strength values are comparable to that for the fields in the resonant reflectors of previously studied SR BWOs [1–3]. Breakdown delay in these devices inspires certain optimism.

Acknowledgements

The work was carried out within framework of the RSF Project No. 21-19-00260. The tests described in Section 2 were performed on the equipment belonging Collective Use Center at the Institute of Electrophysics UB RAS. The authors note a contribution of the Ural Federal University for the possibility of using in the experiments the Tektronix DPO73304D oscilloscope.

5. References

- [1] Korovin S.D., Mesyats G.A., Rostov V.V., Ul'maskulov M.R., Sharypov, K.A., Shpak V.G., Shunailov S.A., Yalandin M.I., *Tech. Phys. Lett.*, **30**(2), 117, 2004; doi: 10.1134/1.1666957
- [2] Rostov V.V., et al., *Phys. Plasmas*, **23**(9), 093103, 2016; doi: 10.1063/1.4962189
- [3] Rostov V.V., et al., *Russian Phys. J.*, **60**(8), 1325, 2017; doi: 10.1007/s11182-017-1216-2
- [4] Vikharev A., Ginzburg N., Kuzikov S., Zotova I., Yalandin M., *European Phys. J. Web of Conferences.*, **195**, 01023, 2018; doi: 10.1051/epjconf/201819501023
- [5] Tarakanov V.P., *User's Manual for Code KARAT*. (Springfield: Berkley Research. Associates Inc., 1992).
- [6] Bratman V.L., Denisov G.G., Korovin S.D., Movshevich B.Z., Polevin S.D., Rostov V.V., Smorgonskii A.V., *Relativistic High-Frequency Electronics. Issue 6*. (Gorky: IPF AN SSSR, 1990. P. 206–216).
- [7] Bratman V.L., Gubanov V.P., Denisov G.G., Korovin S.D., Polevin S.D., Rostov V.V., Smorgonskii A.V., *Pisma v Zh. Tekh. Fiziki*, **4**(1), 9, 1988; <http://journals.ioffe.ru/articles/31043>

- [8] Ginzburg N.S., Malkin A.M., Sergeev A.S., Zheleznov I.V., Zotova I.V., Zaslavsky V.Yu., Boltachev G.Sh., Sharypov K.A., Shunailov S.A., Ul'masculov M.R., Yalandin M.I., *Phys. Rev. Lett.*, **117**, 204801, 2016; doi: 10.1103/PhysRevLett.117.204801
- [9] Ginzburg N.S., Zaslavsky V.Yu., Malkin A.M., Sergeev A.S., Zotova I.V., Sharypov K.A., Shunailov S.A., Shpak V.G., Ul'masculov M.R. Yalandin M.I., *Appl. Phys. Lett.*, **127**, 183505, 2020; doi: 10.1063/5.0026814
- [10] Boltachev G.Sh., Rostov V.V., Sharypov K.A., Shunailov S.A., Shpak V.G., Ulmaskulov M.R., Yalandin M.I., *IEEE Trans. Plasma Sci.*, **43**, 2613, 2015; doi: 10.1109/TPS.2015.2446502
- [11] Mesyats G.A., et al., *Appl. Phys. Lett.*, **116**, 063501, 2020; doi: 10.1063/1.5143486